Influence of Diverse Biases on Network RTK

H.-J. Euler, S. Seeger, F. Takac, *Leica Geosystems AG, Switzerland*

ABSTRACT

The current network RTK messages proposal, the so-called Master-Auxiliary concept, has been outlined in a number of publications (Euler et al., 2001 and Zebhauser et al., 2002). The messages describe the dispersive and non-dispersive errors for a network of reference stations. This information is normally interpolated for the rover's position and applied to reduce the observation errors and improve positioning performance.

Euler et al. (2004) demonstrates the benefits of network RTK corrections in terms of positioning reliability, robustness and accuracy. The data used for the investigation was collected under fair atmospheric conditions. This paper concentrates on data collected during the severe ionospheric conditions recorded in October 2003. The advantage of network RTK information is measured in terms of the percentage of correctly fixed ambiguities.

The Master-Auxiliary concept, as with other network RTK methods, relies on the correct resolution of the integer ambiguities between the reference stations to model the dispersive and non-dispersive network errors. This paper also investigates the influence of incorrectly fixed reference station ambiguities on interpolated network RTK information. Two approximation surfaces are investigated: a linear plane and higher order surface represented by a quadratic function.

INTRODUCTION

The Master-Auxiliary concept uses so-called dispersive and non-dispersive phase correction differences to compress network RTK information without the need for standardized correction models (Euler et al., 2001 and Zebhauser et al., 2002). The correction differences are normally interpolated and applied at the rover to reduce the dispersive and non-dispersive observation errors.

The description of correction differences begins with the following definition of the single difference L1 phase equation $\Delta\Phi^j_{km,1}$ for stations *k (the reference)* and *m (the auxiliary)* and satellite *j*

$$\Delta\Phi^j_{km,1}(t) = \Delta s^j_{km} + \Delta\delta r^j_{km}(t) + c \cdot \Delta dt_{km,1} + \Delta T^j_{km}(t)$$
$$- \frac{\Delta I^j_{km}(t)}{f_1^2} + \frac{c}{f_1} \cdot \Delta N^j_{km,1} + \Delta\varepsilon_1 \quad (1)$$

where

Δs^j_{km}	geometric range term including antenna phase centre variations which have been applied by the network processing software.
$\Delta\delta r^j_{km}$	broadcast orbit error.
Δdt_{km}	receiver clock error.
ΔT^j_{km}	tropospheric refraction error.
ΔI^j_{km}	frequency dependent ionospheric delay.
ΔN^j_{km}	frequency dependent integer ambiguity.
$\Delta\varepsilon$	frequency dependent random measurement error.
t	epoch.
c	speed of light.
f_1	frequency of L1.

Replacing the index of the frequency dependent terms with '2' yields an analogous equation for the L2 single difference phase. Reducing (1) by the slope distance, receiver clock error and the ambiguity term yields the ambiguity-leveled correction difference $\delta\Delta\Phi^j_{km,1}$

$$\delta\Delta\Phi^j_{km,1} = \Delta s^j_{km}(t) - \Delta\Phi^j_{km,1}(t) + c \cdot \Delta dt_{km,1}$$
$$+ \frac{c}{f_1} \cdot \Delta N^j_{km,1} \quad (2)$$

The correction difference described in (2) is separated into a dispersive component, consisting mainly of ionospheric refraction, and a non-dispersive component consisting primarily of tropospheric refraction and orbit errors to reduce the amount of data transmitted to the rover. The equations for the dispersive and non-dispersive components are given in equations (3) and (4) respectively in meters.

$$\delta\Delta\Phi_{km}^{j,\ disp} = \frac{f_2^2}{f_2^2 - f_1^2}\delta\Delta\Phi_{km,1}^{j}$$
$$- \frac{f_2^2}{f_2^2 - f_1^2}\delta\Delta\Phi_{km,2}^{j} \tag{3}$$

$$\delta\Delta\Phi_{km}^{j,\ non-disp} = \frac{f_1^2}{f_1^2 - f_2^2}\delta\Delta\Phi_{km,1}^{j}$$
$$- \frac{f_2^2}{f_1^2 - f_2^2}\delta\Delta\Phi_{km,2}^{j} \tag{4}$$

This alternate representation of the correction differences has some specific benefits. Unlike the correction differences described in (2), changes in the dispersive and non-dispersive components vary at different rates. In general, non-dispersive errors change slowly over time, while dispersive errors vary more rapidly, especially in times of high ionospheric activity. Therefore, optimizing the transmission rates of the dispersive and non-dispersive can maximize data-link throughput.

In addition to the correction differences, the raw carrier phase information for the master reference station, described via RTCM v3.0 standard messages 1003 or 1004 (RTCM 2004), must also be streamed to the rover. Using the phase data of the master station and correction difference, the rover can re-assemble and apply the raw phase information of the auxiliary stations in conventional baseline processing schemes. Alternatively, correction differences can also be interpolated for any position in the network and used to correct rover data.

As with other network RTK methods that model dispersive and non-dispersive errors (e.g. VRS), the Master-Auxiliary concept relies on a common integer ambiguity level for the corrections (Euler et al., 2001). The effect of an ambiguity bias at a reference station on correction differences is the focus of the next section.

INFLUENCE OF INCORRECT AMBIGUITIES ON CORRECTIONS DIFFERENCES

An incorrectly determined single difference ambiguity between a master and auxiliary reference station will manifest itself in the dispersive and non-dispersive correction differences and also in any interpolated correction differences. Table 1 and Table 2 show how an incorrect L1 and/or L2 single difference ambiguity affects the dispersive and non-dispersive correction differences described in (3) and (4) respectively. For simplicity, the magnitude of the ambiguity error is restricted to ± 1 cycle.

ΔN_1 \\ ΔN_2	0	+1	−1
0	0	≈ 1.98	≈ -1.98
+1	≈ -1.54	≈ 0.44	≈ -3.53
−1	≈ 1.54	≈ 3.53	≈ -0.44

Table 1 Impact of a wrong L1 (ΔN_1) and/or L2 (ΔN_2) single difference ambiguity on the dispersive correction difference (in units of L1 cycles).

ΔN_1 \\ ΔN_2	0	+1	−1
0	0	≈ -1.98	≈ 1.98
+1	≈ 2.55	≈ 0.56	≈ 4.53
−1	≈ -2.55	≈ -4.53	≈ -0.56

Table 2 Impact of a wrong L1 (ΔN_1) and/or L2 (ΔN_2) single difference ambiguity on the non-dispersive correction difference (in units of L1 cycles).

The magnitude of the ambiguity error can be amplified in the dispersive and non-dispersive corrections. For example, in the dispersive case (Table 1) a maximum error of ± 3.53 L1 cycles occurs when the incorrect L1 and L2 ambiguities are of equal magnitude but opposite sign. Similarly in the non-dispersive case (Table 2), a maximum error of ± 4.53 L1 cycles also occurs when the error in the L1 and L2 ambiguities are of equal magnitude but opposite sign.

In network RTK, optimal correction differences are normally interpolated for the rover's position. Numerous algorithms can be employed for the interpolation task. For example, Euler et al. (2003) and Euler et al. (2004) compare the effectiveness of a distance weighted interpolation technique with a two-dimensional (2-D) linear plane represented by

$$b_L(x,y) = a_0 + a_1 x + a_2 y \tag{5}$$

where
b_L linear surface.
a_i coefficients defining the plane.
x, y coordinates of the interpolation point.

Higher order approximations are also readily definable. For example, a 2-D quadratic surface can be defined as

$$b_Q(x,y) = a_0 + a_1 x + a_2 y + a_3 x^2 + a_4 xy + a_5 y^2 \tag{6}$$

where
b_Q quadratic surface.

Interpolation algorithms are also sensitive to errors, such as incorrect ambiguities, present in the corrections differences. Figure 1 represents a hypothetical network of 6

reference stations used to analyse the effect of an error at one reference station on the interpolated correction at the rover for two interpolation algorithms: the linear approximation (5) and the quadratic approximation (6).
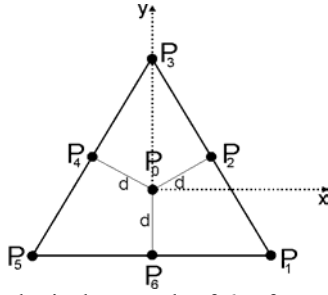
Figure 1 Hypothetical network of 6 reference stations and one rover station located at the centroid of the figure.

Reference stations P_1, P_3 and P_5 lie at the vertices of an equilateral triangle Δ and stations P_2, P_4, and P_6 lie at the midpoints of Δ. Due to the symmetry of the network there are only two scenarios that have to be considered in the analysis: an error introduced at one of the reference stations located at the vertices of Δ (e.g. P_1) and an error introduced at one of the reference stations located at the midpoints of Δ (e.g. P_2).

Let the station coordinates be $P_i = (x_i, y_i)$ where $i = 1,\ldots,6$ for the reference stations and $i = 0$ for the rover station. For simplicity, let $P_0 = (0,0)$. If d is the distance from P_0 to P_2, P_4 and P_6, respectively, then the plane coordinates of the reference stations in Figure 1 are

$$P_1 = \left(\sqrt{3}, -1\right)d, \qquad P_2 = \left(\tfrac{\sqrt{3}}{2}, \tfrac{1}{2}\right)d, \qquad P_3 = (0,2)d$$
$$P_4 = \left(-\tfrac{\sqrt{3}}{2}, \tfrac{1}{2}\right)d, \qquad P_5 = \left(-\sqrt{3}, -1\right)d, \qquad P_6 = (0,-1)d. \tag{7}$$

Let the value given at reference station i (e.g. an L1 or L2 phase correction) be $b_i \in \Re$. We want to approximate the values b_i at (x_i, y_i) by a polynomial function $b(x,y)$ so that

$$b(x_i, y_i) = b_i + \varepsilon_i \tag{8}$$

where ε_i is the approximation error. The linear approximation given in (5) can be rewritten as

$$b_L(x,y) = (1,x,y) \bullet (a_0, a_1, a_2)^t \tag{9}$$

and the quadratic case (6) as

$$b_Q(x,y) = (1,x,y,x^2,xy,y^2) \bullet (a_0,a_1,a_2,a_3,a_4,a_5)^t \tag{10}$$

Expanding the polynomial equation (8) for all i results in

$$M_L \bullet (a_0, a_1, a_2)^t = b + \varepsilon_L \tag{11}$$

where

$$M_L = \begin{pmatrix} 1 & x_1 & y_1 \\ 1 & x_2 & y_2 \\ 1 & x_3 & y_3 \\ 1 & x_4 & y_4 \\ 1 & x_5 & y_5 \\ 1 & x_6 & y_6 \end{pmatrix}, \quad b = \begin{pmatrix} b_1 \\ b_2 \\ b_3 \\ b_4 \\ b_5 \\ b_6 \end{pmatrix}, \quad \varepsilon_L = \begin{pmatrix} \varepsilon_1 \\ \varepsilon_2 \\ \varepsilon_3 \\ \varepsilon_4 \\ \varepsilon_5 \\ \varepsilon_6 \end{pmatrix}$$

for the linear equation (9). For brevity, the expansion of (8) for the quadratic case is not given here.

For the linear case, the polynomial coefficients $a_L \equiv (a_0, a_1, a_2)^t$ are given by

$$a_L = \left(M_L^t M_L\right)^{-1} M_L^t b \tag{12}$$

An analogous equation for the quadratic polynomial coefficients a_Q is obtained by substituting the subscript 'L' in (12) with 'Q'.

Substituting (x_i, y_i) from (7) into M_L yields the following expression for $\left(M_L^t M_L\right)^{-1} M_L^t$:

$$\left(M_L^t M_L\right)^{-1} M_L^t = \begin{pmatrix} \tfrac{1}{6} & \tfrac{1}{6} & \tfrac{1}{6} & \tfrac{1}{6} & \tfrac{1}{6} & \tfrac{1}{6} \\ \tfrac{2\sqrt{3}}{15d} & \tfrac{\sqrt{3}}{15d} & 0 & -\tfrac{\sqrt{3}}{15d} & -\tfrac{2\sqrt{3}}{15d} & 0 \\ -\tfrac{2}{15d} & \tfrac{1}{15d} & \tfrac{4}{15d} & \tfrac{1}{15d} & -\tfrac{2}{15d} & -\tfrac{2}{15d} \end{pmatrix} \tag{13}$$

Again the corresponding quadratic equation is omitted for brevity. Assume that the values b_i differ from the correct values $\bar{b}_i$ by Δb_i, i.e. $b_i = \bar{b}_i + \Delta b_i$. Substituting $\bar{b} + \Delta b = (\bar{b}_1 + \Delta b_1, \ldots, \bar{b}_6 + \Delta b_6)^t$ into (12) leads to a natural splitting of the polynomial coefficients a_L into terms $\bar{a}_L$ belonging to $\bar{b}$ and terms Δa belonging to Δb. We explicitly write down this separation of the polynomial coefficients for the linear case

$$a_L = \left(M_L^t M_L\right)^{-1} M_L^t \left(\bar{b} + \Delta b\right)$$
$$\overset{!}{=} \bar{a}_L + \Delta a_L \tag{14}$$

where $\bar{a}_L = \left(M_L^t M_L\right)^{-1} M_L^t \bar{b}$ and

$$\Delta a_L = \left(M_L^t M_L\right)^{-1} M_L^t \Delta b \tag{15}$$

For the quadratic case Δa_Q is given by

$$\Delta a_Q = \left(M_Q^t M_Q\right)^{-1} M_Q^t \Delta b \qquad (16)$$

Thus, following from (9) and (10), the change in the approximated value at $P = (x, y)$ due to the reference station biases Δb is given by

$$\Delta b_L(x, y) = (1, x, y) \bullet \Delta a_L \qquad (17)$$

for the linear case and

$$\Delta b_Q(x, y) = (1, x, y, x^2, xy, y^2) \bullet \Delta a_Q \qquad (18)$$

for the quadratic case. The analysis is restricted to the following two cases:

Case 1: error δ introduced at P_1, i.e. $\Delta b = (\delta, 0, 0, 0, 0, 0)^t$

Case 2: error δ introduced P_2, i.e. $\Delta b = (0, \delta, 0, 0, 0, 0)^t$

Substituting Δb for case 1 and case 2 into (15) and (16) yields the following general expressions for the change in the approximated value $P = (x, y)$:

Case 1:

$$\Delta b_L(x, y) = (1, x, y) \bullet \left(\frac{1}{6}, \frac{2\sqrt{3}}{15d}, -\frac{2}{15d}\right)^t \delta \qquad (19)$$

$$\Delta b_Q(x, y) = (1, x, y, x^2, xy, y^2) \bullet$$
$$\left(-\frac{1}{9}, \frac{\sqrt{3}}{18d}, -\frac{1}{18d}, \frac{1}{6d^2}, -\frac{\sqrt{3}}{9d^2}, \frac{1}{18d^2}\right)^t \delta \qquad (20)$$

Case 2:

$$\Delta b_L(x, y) = (1, x, y) \bullet \left(\frac{1}{6}, \frac{\sqrt{3}}{15d}, \frac{1}{15d}\right)^t \delta \qquad (21)$$

$$\Delta b_Q(x, y) = (1, x, y, x^2, xy, y^2) \bullet$$
$$\left(-\frac{4}{9}, \frac{2\sqrt{3}}{9d}, -\frac{2}{9d}, 0, \frac{2\sqrt{3}}{9d^2}, -\frac{2}{9d^2}\right)^t \delta \qquad (22)$$

For the rover station $P_0 = (0, 0)$, located at the centre of the network, (19), (20), (21) and (22) reduce to the following simplified expressions

Case 1: $\Delta b_L(0, 0) = \frac{1}{6}\delta$, $\Delta b_Q(0, 0) = -\frac{1}{9}\delta$

Case 2: $\Delta b_L(0, 0) = \frac{1}{6}\delta$, $\Delta b_Q(0, 0) = -\frac{4}{9}\delta$

Thus, the influence of a bias at P_1, P_3 or P_5 (case 1) on the interpolated value at P_0 for the quadratic approximation is only $\frac{2}{3}$ of the influence for the linear approximation. However, a bias at P_2, P_4, or P_6 (case 2) causes, in the linear case, an error in the interpolated value at P_0 that is only $\frac{3}{8}$ of the magnitude of the quadratic approximation. Figure 2, Figure 3 and Figure 4, illustrate the interpolated error for any station $P = (x, y)$ for each case with $d = \delta = 1$.
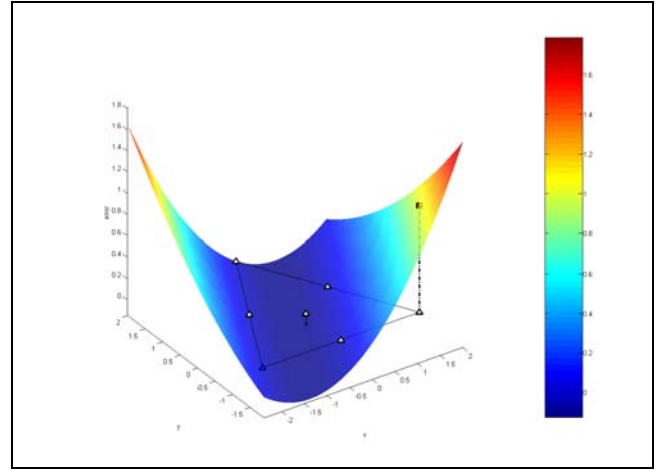
Figure 2 Case 1 (quadratic approximation): the interpolated error at a station $P = (x, y)$ resulting from a bias at one of the reference stations P_1, P_3 or P_5.
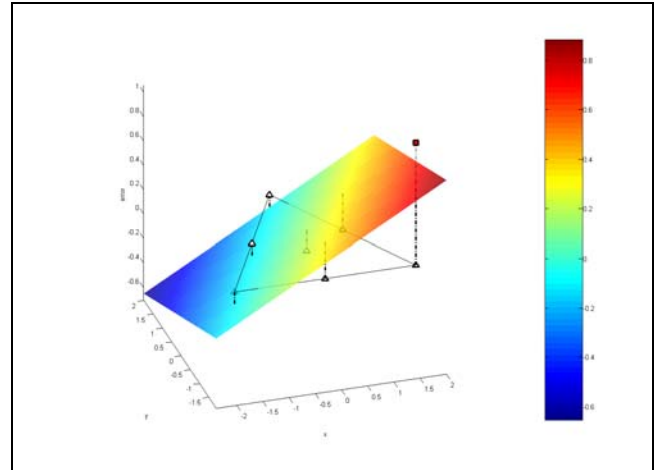
Figure 3 Case 1 (linear approximation): the interpolated error at a station $P = (x, y)$ resulting from a bias at one of the reference stations P_1, P_3 or P_5.
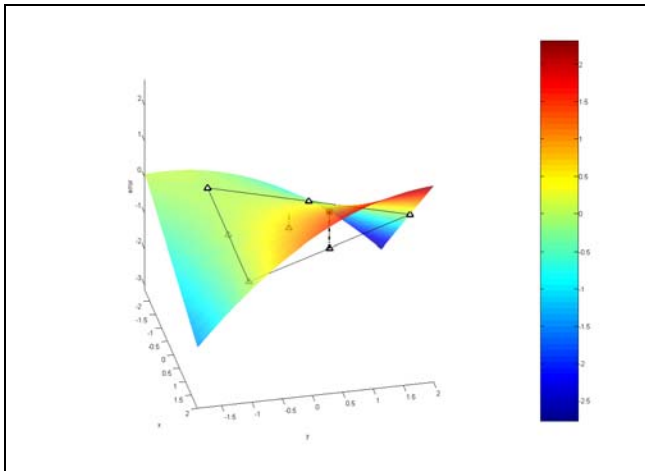
Figure 4 Case 2 (quadratic approximation): the interpolated error at station $P = (x, y)$ resulting from a bias present at one of the reference stations P_2, P_4, or P_6.

For the network described in Figure 1, the interpolated error at the central station P_0 is always reduced for both the linear and quadratic approximations in comparison to the magnitude of the error at the reference station. However, other network configurations of 6 reference stations (the minimum number of stations necessary for a quadratic approximation) were analysed where the quadratic approximation amplifies the introduced error at the centre of the network. For example, Figure 5 demonstrates the results for a network of reference stations placed on a circle around the rover station. Since an exact circle results in a singular configuration for the quadratic approximation, one of the reference stations is slightly shifted away from an exact circle.
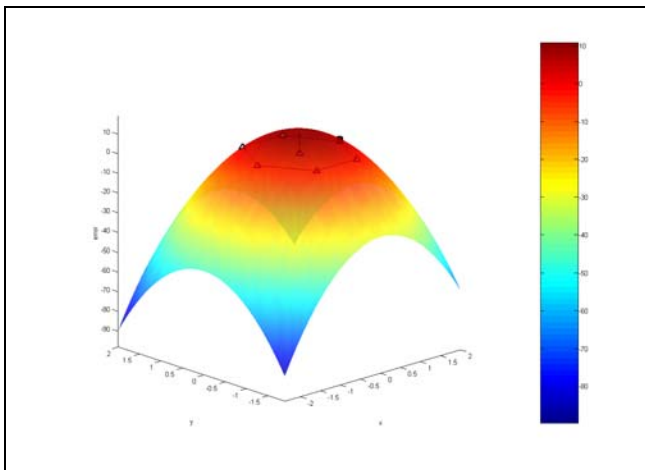
Figure 5 The interpolated error at a station $P = (x, y)$ resulting from a bias one reference station for the quadratic approximation.

The amplification of the error at P_0 is visually apparent (value is much greater than the reference station bias $\delta = 1$). In contrast to the quadratic case, the linear approximation always attenuates the introduced error by a factor of about $1/n$ where n is the number of stations used in the network.

Due to the higher sensitivity in many cases of the quadratic approximation to errors in reference station data and to the many singular network configurations we have recognized in our investigations (but not detailed here), the 2-D linear approximation is used for in the remaining empirical analysis which focuses on the effects of the ionosphere of network RTK corrections.

ANALYSIS OF THE EFFECT OF HIGH IONOSPHERE ON NETWORK RTK

For a network of 7 stations located in Bavaria, Germany, 8 hours of 1 Hz data were collected on the 31st October 2003 during a period of known high ionospheric activity (IPS Radio and Space Services, 2003). The stations depicted in Figure 6 form a part of the SAPOS permanent reference station network.
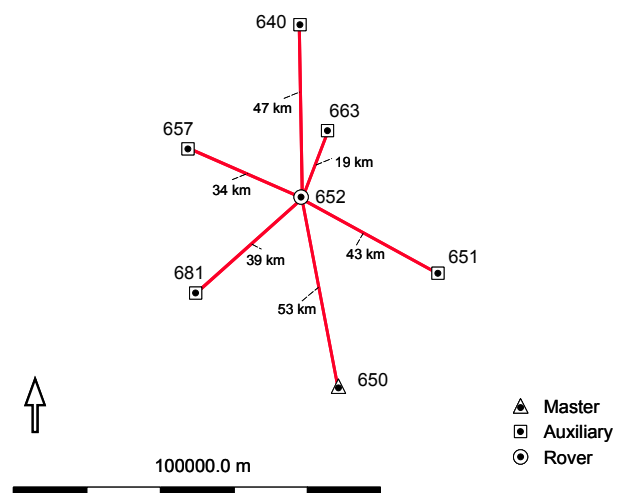
Figure 6 Distribution of auxiliary reference stations in relation to the rover station 652. Station 663 was the designated master reference station.

Cycle slips were removed from the raw data prior to the estimation of the double-differenced phase ambiguities between the reference stations. The resulting ambiguity-leveled data was used to form RTCM type 20 phase corrections for each reference station. Station 663 represents the master reference station. The remaining stations serve as auxiliaries, except for station 652, which is the designated rover. The length of the master-rover baseline is 19km, which represents the shortest baseline in the network.

The data set was divided into two periods for the empirical analysis: 00:00–04:00am and 04:00am–08:00am. For these two periods, double-difference dispersive and non-dispersive phase residuals were computed for the master-rover baseline.

The magnitude and behavior of the non-dispersive errors for both periods are typical of the numerous baselines presented in the work of Euler et al. (2004), Euler and

Zebhauser (2003) and Euler et al. (2003). Therefore, plots of the non-dispersive errors are not explicitly presented here.

The dispersive errors scaled to L1 cycles for the period 00:00 – 04:00am are shown in Figure 7.
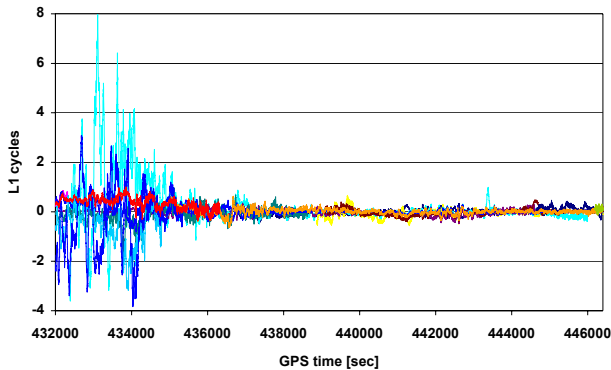
Figure 7 Dispersive errors short baseline (663 – 652, 00:00 – 04:00am).

A relatively large disturbance of the dispersive errors is evident in the first hour of the plot. Excursions of approximately 8 cycles are present during this burst. In contrast, the magnitude of dispersive errors in the second half of the plot is generally less than ±1 cycle. The disruption of the dispersive errors early in the data set is attributed to the high ionospheric activity present during the period of data collection.

The dispersive errors scaled to L1 cycles for the period 04:00 – 08:00am are shown in Figure 8.
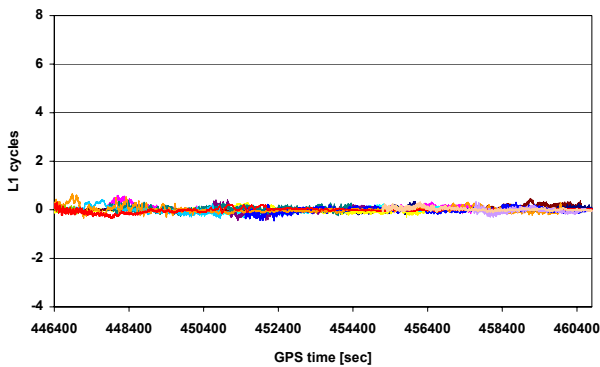
Figure 8 Dispersive errors for the baseline 663 – 652 (04:00 – 08:00am).

The magnitude of the dispersive errors in this is generally less than ±1 cycle. In contrast to the period 00:00 – 04:00am, no anomalous excursions of the errors are present. In general, the magnitude of the dispersive errors for the entire data set (00:00 – 08:00am) is relatively high. As a comparison, the magnitude of dispersive errors for a 94km baseline presented in Euler et al. (2004) was generally less than ±1 cycle. The master-rover baseline in this network is 19km, which is approximately 5 times shorter,

yet the magnitude of the dispersive errors is of similar order.

The dispersive and non-dispersive errors were grouped into elevation bins of 1 degree according to the elevation of the lowest satellite used to build the double difference. For each elevation bin, the average and mean true error was calculated. The mean true error $\bar{\varepsilon}$ is given by

$$\bar{\varepsilon} = \sqrt{\frac{[\varepsilon\varepsilon]}{n}} \qquad (7)$$

where ε is the true error and n is the number of observations. Figure 9 and Figure 10 show the average and mean true non-dispersive errors for the periods 00:00 – 04:00am and 04:00 – 08:00am respectively.
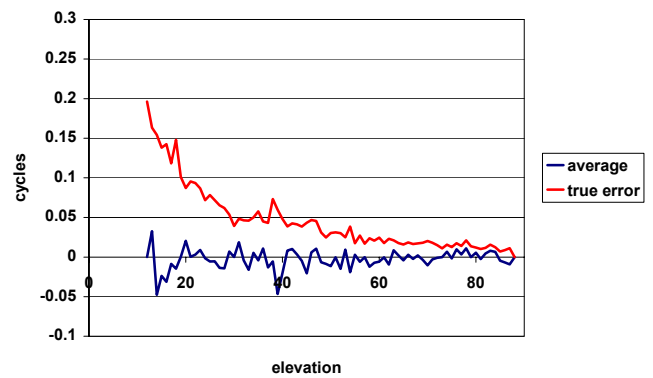
Figure 9 Uncorrected average and true non-dispersive errors for the baseline 663 – 652 (00:00 – 04:00am).
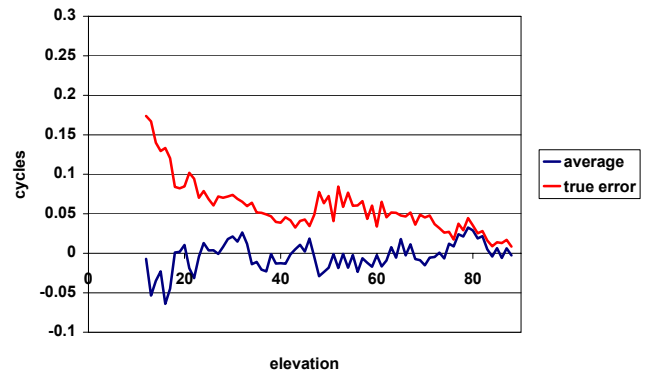
Figure 10 Uncorrected average and true non-dispersive errors for the baseline 663 – 652 (04:00 – 08:00am).

Again the magnitude and behavior of the non-dispersive errors is typical of previous analysis (Euler et al., 2004 and Euler and Zebhauser, 2003). The errors are apparently random as illustrated by the average error in both figures. The magnitude of the errors increases for satellites below 20°, which is due to unmodeled geometric biases e.g. residual troposphere.

Of particular interest in this paper is the effect of the ionosphere. Figure 11 shows the average and true dispersive errors for the period 00:00 – 04:00am.
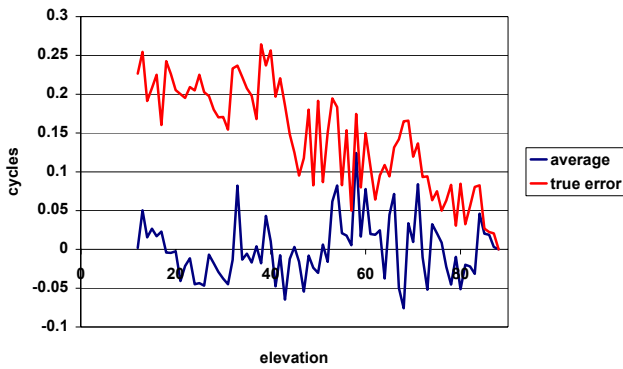
Figure 11 Uncorrected average and true dispersive errors for the baseline 663 – 652 (00:00 – 04:00am).

The apparent random nature of the average dispersive error suggests that no elevation dependent (dispersive) biases are present in the data set. In general, the magnitude of the errors tends to be greater for low elevation satellites as illustrated by the true error plot. However, two anomalies are evident between approximately 10° and 40° and between 45° and 70°. In these two regions, the dispersive errors tend not to decrease with increasing elevation.

Figure 12 plots the average and mean true dispersive errors for the second period 04:00 – 08:00am.
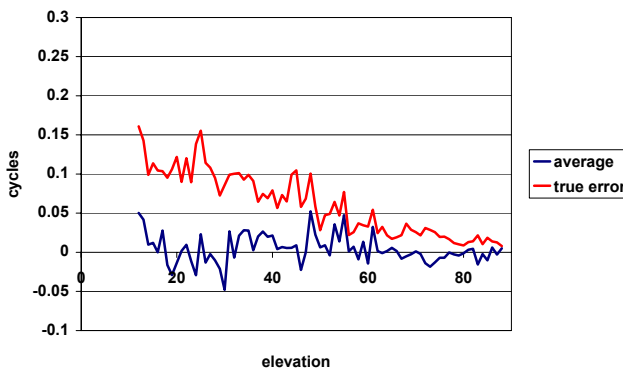
Figure 12 Uncorrected average and true dispersive errors for the baseline 663 – 652 (04:00 – 08:00am).

The results are characteristic of the behavior of dispersive errors seen in previous work (Euler et al., 2004 and Euler and Zebhauser, 2003). The magnitude of the errors during this time range from approximately 0 to 0.15 cycles as opposed to 0 – 0.26 cycles for the period 00:00 – 04:00am (Figure 11). The average dispersive error is apparently random and the magnitude of the error decreases linearly with increasing elevation.

The goal of network RTK corrections is to reduce the magnitude of the observation errors at the rover station. To measure this improvement, dispersive and non-dispersive corrections for the rover position (663) were interpolated from a 2-D linear plane fitted to the estimated dispersive and non-dispersive errors of all 6 reference stations. An update rate of 15 seconds was adopted for the non-dispersive correction differences, as proposed in RTCM SC104. The high level of ionospheric activity, as demonstrated in Figure 7, enforced the use of a 2-second update rate for the dispersive contribution. The interpolated corrections were applied to the rover data and the corrected double-difference phase errors computed. Figure 13 shows the corrected dispersive and non-dispersive errors for the period 00:00 – 04:00am.
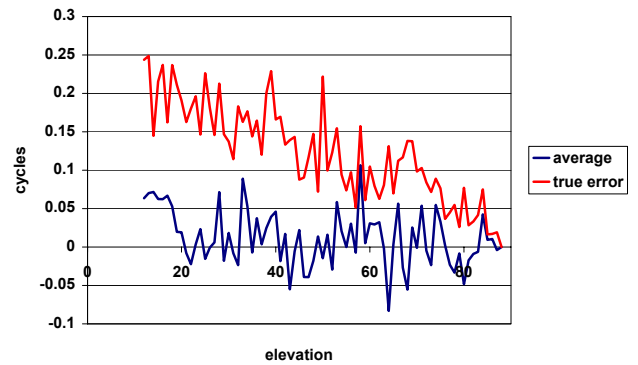
Figure 13 Corrected average and true dispersive errors of the baseline 663 – 652 (00:00 – 04:00am). The corrections were interpolated from a 2D plane surface fitted to the estimated dispersive errors of 6 reference stations.

The dispersive errors are still apparently random. In comparison to Figure 11, the magnitude of the errors decrease linearly with increasing elevation. However, the average and true error plots still exhibit a high degree of noise in comparison to the corrected dispersive errors for the second period (04:00 – 08:00am) shown in Figure 14.
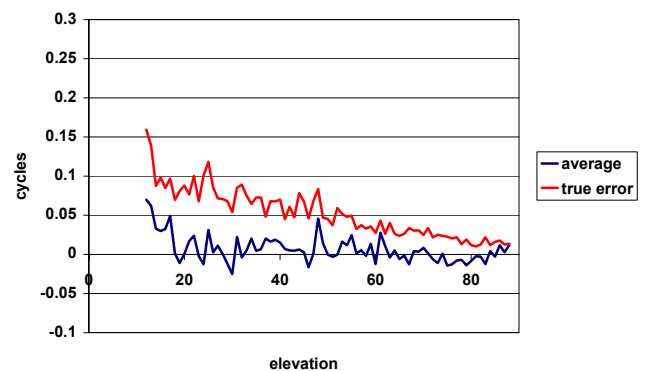
Figure 14 Corrected average and true dispersive errors of the baseline 663 – 652 (04:00 – 08:00am). The corrections were interpolated from a 2D plane surface fitted to the estimated dispersive errors of 6 reference stations.

In general, the magnitude of the dispersive errors is reduced in both periods. Figure 15 explicitly quantifies the magnitude of the improvement for the period 00:00 – 04:00am.
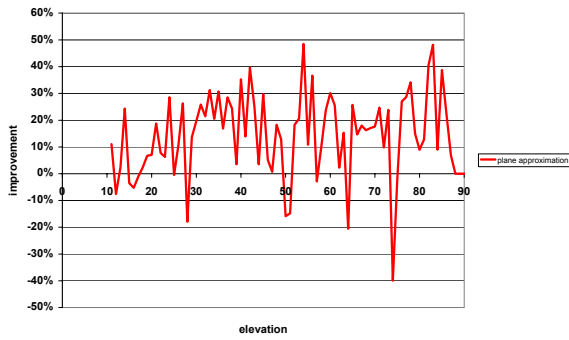
Figure 15 Improvement in the magnitude of the dispersive true errors of the corrected baseline 663 – 652 (00:00 – 04:00am). The network corrections were interpolated from a plane surface fitted to the estimated dispersive errors of 6 reference stations.

The interpolated corrections reduce approximately 20%-40% of the dispersive effects over all elevation bins. The improvements are less significant than those shown previously in Euler et al. (2003) and Euler et al. (2004). The effectiveness of interpolation techniques relies on the spatial correlation of the dispersive errors in the network. However, the ionospheric burst visible during this period (Figure 7) is thought to be local resulting in a spatial de-correlation of the dispersive errors. This assertion is currently the subject of ongoing research. In this case, network RTK corrections are not expected to significantly improve processing results for this period.

BASELINE PROCESSING RESULTS

The baseline 663 – 652 (Figure 6) was processed with and without applied network corrections using observation periods of 45, 60 and 90-second observation times and a 10-degree elevation mask for both data periods. The network corrections were interpolated from a plane surface fitted to the estimated dispersive errors of 6 reference stations. The percentage of fixed ambiguities was used as the measure of processing performance.

As hypothesized in the previous section, network corrections applied to the rover data failed to significantly improve the number of correctly fixed ambiguities for the period 00:00 – 04:00am. In contrast, Figure 16 shows the percentage of correctly fixed ambiguities for the data period 04:00 – 08:00am when no ionospheric bursts were observed.
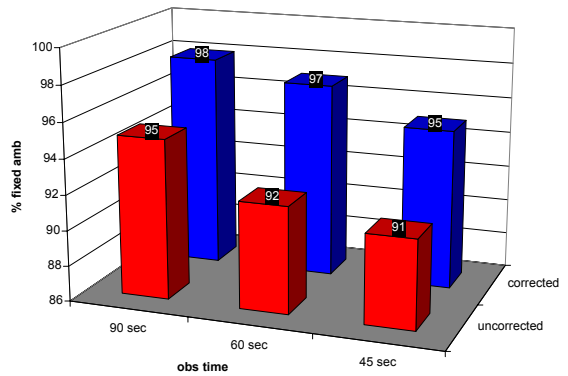
Figure 16 Percentage of fixed solutions for the corrected and uncorrected baseline 663 – 652 (04:00 – 08:00am) using 90 second, 60 second and 45 second observation periods and a 10-degree elevation mask.

Network corrections improved processing performance for all the observation times tested during the period 04:00 – 08:00am. Even during the relatively high ionosphere activity, more than 95% of ambiguities could be fixed with observation times of 45 seconds or more.

CONCLUSIONS

A theoretical study on the impact of incorrect ambiguities on correction differences showed that L1 and L2 ambiguity biases might be amplified in dispersive and non-dispersive correction differences. These biases also manifest themselves in the interpolated corrections. Two two-dimensional approximation surfaces, a linear plane and a quadratic surface, were tested to assess the influence of a reference station bias on interpolated corrections. The quadratic approximation proved to be more sensitive to network geometry and in some cases even amplified the error present at the reference station. The linear plane approximation is more robust and always attenuates the reference station error by a factor of 1/n where *n* is the number of stations in the network.

An empirical study was undertaken to measure the performance of network RTK during periods of high ionospheric activity. An analysis of the dispersive errors present in the test data illustrated the presence of large ionospheric disturbances including a so-called ionospheric burst. The disturbed ionospheric condition enforced a 2-second sampling rate of the dispersive corrections to be adopted for the tests.

Network corrections did not significantly improve RTK performance, measured in terms of the percentage of correctly fixed ambiguities, in the period when the ionospheric burst was observed. It is expected that the burst was localized resulting in a spatial de-correlation of the dispersive errors. In this case, interpolation methods will not be successful at modeling the true behavior of dispersive errors in the network. This is the subject of further research.

In contrast, network corrections improved processing performance for all the observation times tested in the period not containing the ionospheric burst. More than 95% of ambiguities could be fixed with observation times of 45 seconds or more.

ACKNOWLEDGEMENTS

REFERENCES

Euler, H.-J., Keenan, C.R., Zebhauser, B. E., Wübbena, G. (2001): Study of a Simplified Approach in Utilizing Information from Permanent Reference Station Arrays, ION GPS 2001, September 11-14, 2001, Salt Lake City, UT

Euler, H.-J., Zebhauser, B. E., Townsend, B., Wübbena, G. (2002): Comparison of Different Proposals for Reference Station Network Information Distribution Formats, ION GPS 2002, September 24-27, 2002, Portland, OR

Euler, H.-J., Zebhauser, B.E. (2003): The Use of Standardized Network RTK Messages in Rover Applications for Surveying, ION NTM 2003, January 22-24, 2003, Anaheim, CA

Euler, H.-J., Seeger, S., Zelzer, O., Takac, F., Zebhauser, B. E. (2004): Improvement of Positioning Performance Using Standardized Network RTK Messages, ION NTM 2004, January 26-28, 2004, San Diego, CA

IPS Radio and Space Services (2003): A Remarkable Period of Space Weather October-November 2003, available at:
http://www.ips.gov.au/Category/Educational/Space%20Weather/Space%20Weather%20Effects/oct-nov-03-activity.pdf (accessed: 16th August 2004).

RTCM (2004): RTCM Recommended Standards for Differential GNSS (Global Navigation Satellite Systems) Service, Version 3.0, RTCM paper 30-2004-SC104-STD.

Zebhauser, B. E., Euler, H.-J., Keenan, C.R., Wübbena, G. (2002): A Novel Approach for the Use of Information from Reference Station Networks Conforming to RTCM V2.3 and Future V3.0, ION NTM 2002, January 28-30, 2002, San Diego, CA